Bioorganic & Medicinal Chemistry 19 (2011) 4782–4795

Contents lists available at ScienceDirect

Bioorganic & Medicinal Chemistry

journal homepage: www.elsevier.com/locate/bmc

Synthesis and antiproliferative activity of novel 2-aryl-4-benzoyl-imidazole derivatives targeting tubulin polymerization

Jianjun Chen [a], Chien-Ming Li [b], Jin Wang [a], Sunjoo Ahn [b], Zhao Wang [a], Yan Lu [a], James T. Dalton [b], Duane D. Miller [a,b], Wei Li [a,*]

[a] Department of Pharmaceutical Sciences, College of Pharmacy, University of Tennessee Health Science Center, Memphis, TN 38163, USA
[b] GTx Inc., Memphis, TN 38163, USA

ARTICLE INFO

Article history:
Received 8 April 2011
Revised 24 June 2011
Accepted 28 June 2011
Available online 1 July 2011

Keywords:
2-Aryl-4-benzoyl-imidazoles
Cancer drug resistance
Melanoma
Prostate cancer

ABSTRACT

We previously reported the discovery of 2-aryl-4-benzoyl-imidazoles (ABI-I) as potent antiproliferative agents for melanoma. To further understand the structural requirements for the potency of ABI analogs, gain insight in the structure–activity relationships (SAR), and investigate metabolic stability for these compounds, we report extensive SAR studies on the ABI-I scaffold. Compared with the previous set of ABI-I analogs, the newly synthesized ABI-II analogs have lower potency in general, but some of the new analogs have comparable potency to the most active compounds in the previous set when tested in two melanoma and four prostate cancer cell lines. These SAR studies indicated that the antiproliferative activity was very sensitive to subtle changes in the ligand. Tested compounds **3ab** and **8a** are equally active against highly paclitaxel resistant cancer cell lines and their parental cell lines, indicating that drugs developed based on ABI-I analogs may have therapeutic advantages over paclitaxel in treating resistant tumors. Metabolic stability studies of compound **3ab** revealed that *N*-methyl imidazole failed to extend stability as literature reported because de-methylation was found as the major metabolic pathway in rat and mouse liver microsomes. However, this sheds light on the possibility for many modifications on imidazole ring for further lead optimization since the modification on imidazole, such as compound **3ab**, did not impact the potency.

1. Introduction

Cancer is the second leading cause of death in the world, ranked after only heart disease.[1] Of the many clinically useful anticancer agents, drugs targeting tubulin polymerization (e.g., paclitaxel, docetaxel, and vinblastine) have enjoyed wide success in treating various types of cancers, including prostate cancer and melanoma.[2–4] However, the prolonged use of those tubulin-targeting agents often results in drug resistance in cancer cells, especially P-glycoprotein (Pgp)-mediated multidrug resistance.[5–7] The development of multidrug resistance to tubulin inhibitors severely limits their efficacy; therefore, novel tubulin inhibitors that can effectively overcome drug resistance could significantly improve their clinical efficacy.[8,9]

We recently reported a series of 2-aryl-4-benzoyl-imidazole (ABI-I) analogs targeting the colchicine binding site in tubulin as potent antiproliferative agents for melanoma and prostate cancer.[10] Compared with existing tubulin-targeting agents such as paclitaxel, colchicine, or vinblastine, the ABI-I compounds have comparable in vitro and in vivo potency but can effectively circumvent Pgp-mediated drug resistance.[10] ABI-I was designed using the imidazole moiety as a biomimetic replacement of the central thiazole ring of 4-substituted methoxybenzoyl-aryl-thiazole (SMART) (Fig. 1).[10] Compared with SMART analogs,[11] ABI-I compounds have improved water solubility, pharmacokinetic (PK) properties, and oral bioavailability without compromising activity.[12] The activity of ABI-I analogs depends strongly on the nature of the substitutions on the aromatic A and C rings (Fig. 1). We also found that the benzene sulfonyl protecting group on the N1-position of the imidazole scaffold does not affect potency. To further understand the structural requirements for the potency of ABI analogs, to gain insight in the structure–activity relationships (SAR), and to investigate metabolic stability for these compounds, we performed additional SAR studies on the ABI-I scaffold.

In this paper, we report the synthesis and biological studies of ABI-II analogs (Fig. 2). Specifically, we modified the structures of the ABI-I by (1) converting the A ring of ABI-I from a phenyl ring to an indole ring to understand the tolerability of the A ring modification (**ABI-II-1**); (2) introducing various substituents on

Abbreviations: ABI, 2-aryl-4-benzoyl-imidazoles; BCRP, breast cancer resistance protein; MDR, multidrug resistance; MRP, multidrug resistance-associated proteins; Pgp, P-glycoprotein; SAR, structure–activity relationships; SMART, 4-substituted methoxybenzoyl-aryl-thiazole; TMS, tetramethylsilane.

* Corresponding author. Tel.: +1 (901) 448 7532; fax: +1 (901) 448 6828.
E-mail address: wli@uthsc.edu (W. Li).

0968-0896/$ - see front matter © 2011 Elsevier Ltd. All rights reserved.
doi:10.1016/j.bmc.2011.06.084

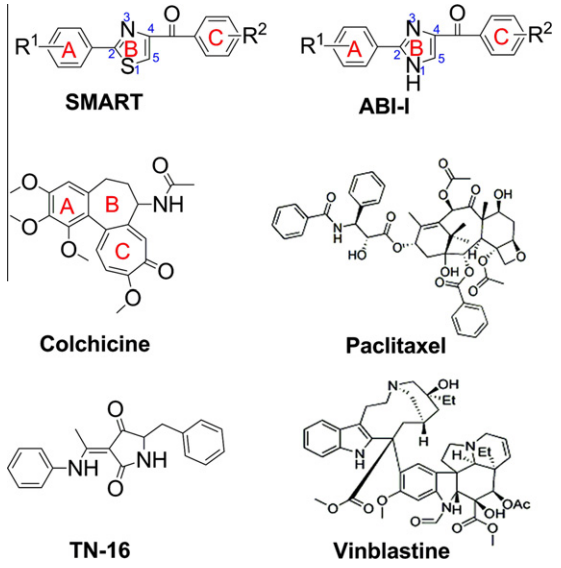

Figure 1. Structures of tubulin binders.

the N1-position of the imidazole ring to understand the effects of different groups on activity (**ABI-II-2**); (3) demethylating the *para*-methoxy group on the C ring to understand its effect on antiproliferative activity (**ABI-II-3**); (4) fusing the A and B rings to understand the importance of relative geometry between them (**ABI-II-4**), inspired by the highly active compounds (picomolar potency, compound **15**, Fig. 2) recently reported[13] and by the same analogs that also target tubulin with IC_{50} values in the nanomolar range.[14] We also conducted in vitro metabolic stability studies for **3ab** (an **ABI-II-2** analog), one of the best compounds in ABI-II, and the result unveiled the vulnerable sites of ABI-II and provided direction for future modifications on the imidazole ring to obtain further optimized PK profiles.

2. Chemistry

The synthesis of compounds **2**(**a, c**) and **3**(**aa, ab, b**) is summarized in Scheme 1. Compound **1**(**a–c**) was synthesized according to our previously reported procedures.[10] Treatment of **1**(**a, c**) with aluminum chloride provided the *para*-demethylated compound **2**(**a, c**) with the 3,5-dimethoxy intact. Compound **3aa** was prepared by benzylation of the N-1 position of **1a**, while methylation of the N-1 position of **1a** and **1b** afforded compounds **3ab** and **3b**, respectively.

Compounds **7b** and **8a** were synthesized following our established method[10] as outlined in Scheme 2. The substituted benzaldehyde compound **4**(**a, b**) was converted to compound **5(a, b)** in the presence of ammonium hydroxide and glyoxal to construct the imidazole scaffold. The imidazole ring of compound **5**(**a, b**) was protected by an appropriate phenylsulfonyl group followed by coupling with substituted benzoyl chloride to achieve compound **7(a, b)**. Treating compound **7a** with *tert*-butylammonium fluoride to remove the protecting group afforded compound **8a**. The synthesis of compounds **12(a–h)** and **13(aa, ab, b)**, as well as of **14(a, b)**, is described in Scheme 3. Protecting the indole or benzimidazole NH of compounds **9**(**a–h**) with a phenylsulfonyl moiety yielded intermediates **10**(**a–h**), which were deprotonated by *tert*-butyllithium followed by coupling with the 3,4,5-trimethoxy benzoyl chloride to generate compounds **11**(**a–h**). Removing the protecting group from **11**(**a–h**) gave compound **12**(**a–h**). Compounds **12a** and **12b** were methylated by methyliodide to obtain compounds **13aa** and **13b**, respectively. Benzylating compound **12a** provided compound **13ab**. The synthesis of compounds **15a** and **15b** was straightforward with a one-step reaction involved. The commercial starting materials **14a** and **14b** were treated directly by *tert*-butyllithium followed by benzoylation to achieve the desired products **15a** and **15b**. Compound **15aa** (see Table 1 infra for structure) was separated as a side product from the synthesis of compound **15a**.

The synthesis of compound **21b** is outlined in Scheme 4. This route was originally designed for the synthesis of **21a**, but the

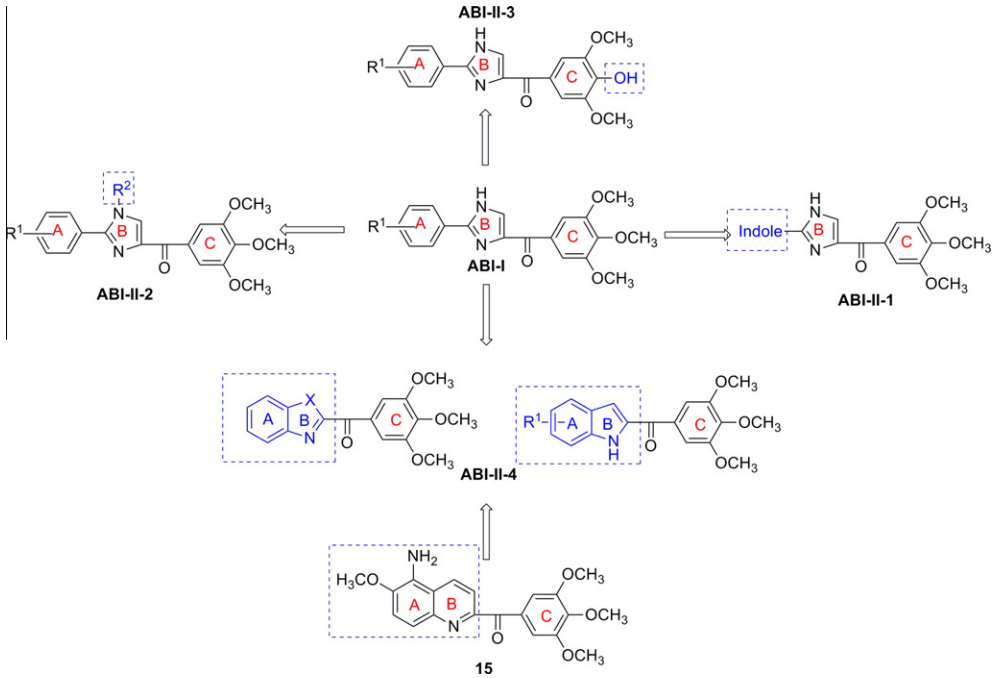

Figure 2. Design protocol for the ABI-II analogs (changes are indicated in blue).

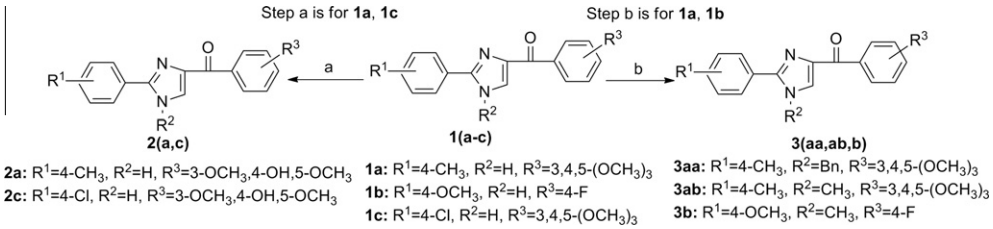

Scheme 1. Reagents and conditions: (a) $AlCl_3$, THF, reflux; (b) NaH, CH_3I for **3ab** and **3b** and BnBr for **3aa**, THF, reflux.

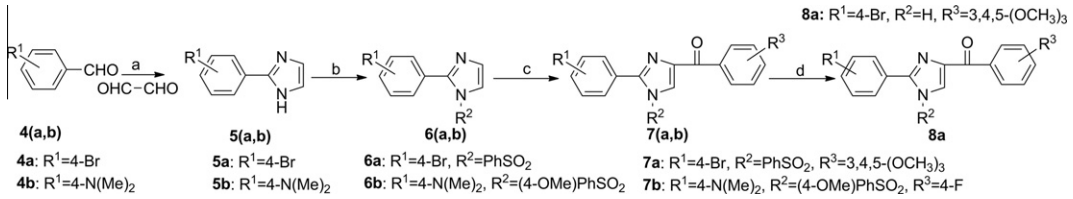

Scheme 2. Reagents and conditions: (a) NH_4OH, ethanol, glyoxal, rt; (b) NaH, substituted $PhSO_2Cl$, THF, 0 °C–rt; (c) *t*-BuLi (1.7 M in pentane), substituted benzoyl chloride, THF, −78 °C; (d) Bu_4NF, rt.

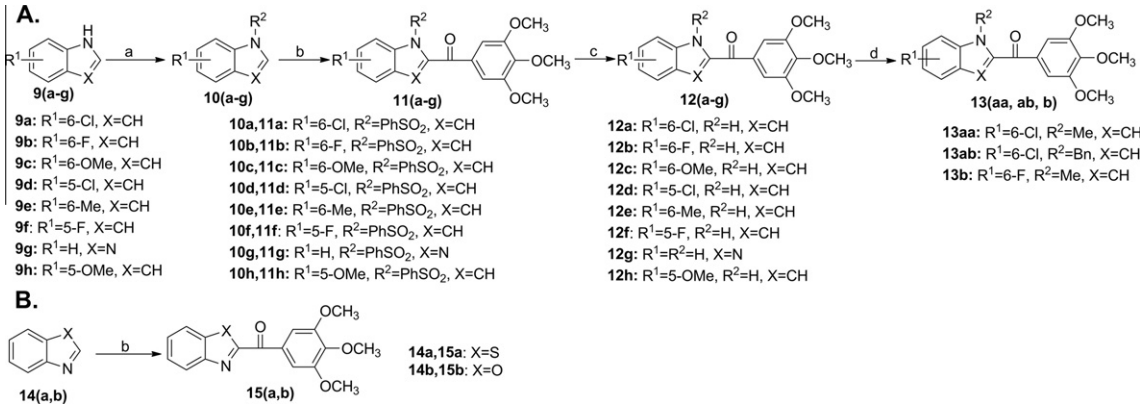

Scheme 3. Reagents and conditions: (a) NaH, $PhSO_2Cl$, THF, 0 °C–rt; (b) *t*-BuLi (1.7 M in pentane), benzoyl chloride, THF, −78 °C; (c) NaOH, ethanol, H_2O, reflux; (d) NaH, CH_3I for **13aa** and **13b** or BnBr for **13ab**, THF, reflux.

nonselectivity of the benzoylation at the indole-2 and imidazole-4 positions resulted in the formation of compound **21b**, which is a closely related but bulkier analog of **20a**. Briefly, the indole-5-carboxaldehyde compound **16** was protected by the phenylsulfonyl group on the indole NH to afford intermediate **17**.[15] Compound **17** was reacted with glyoxal and ammonium hydroxide to generate the 2-aryl-imidazole compound **18**. Protecting the imidazole NH with phenylsulfonyl gave the intermediate **19**, which was coupled with 3,4,5-trimethoxy benzoyl chloride to produce compound **20b**. Removing the protecting group from **20b** provided compound **21b**.

3. Antiproliferative activities of ABI-II against melanoma and prostate cancer cells

The antiproliferative activity of these compounds was evaluated in two human metastatic melanoma cell lines (A375 and WM164) and four human prostate cancer cell lines (LNCaP, PC-3, Du 145, and PPC-1) by using the methods described previously.[10,16] Colchicine was used as a positive control. The ability of these new analogs to inhibit the growth of cancer cell lines is summarized in Table 1.

3.1. Effects of A ring modifications (ABI-II-1)

For compounds with A ring modification, compound **8a** (Table 1, 0.04 μM, unless specified, the IC_{50} value for each compound is the average IC_{50} value obtained from all six cancer cell lines) showed comparable activity with its chlorine counterpart compound **1c** (Fig. 3, 0.03 μM, all the compounds in Fig. 3 were previously reported as ABI-I analogs),[10] indicating that a bromine on the *para*-position of the A ring is well tolerated. Compound **21b** (Table 1, 2.9 μM), with a 2-benzoylated indole as the A ring, showed moderate activity, which is consistent with our observation in the previous set of ABIs that a bulky A ring reduces activity,[10] suggesting that the size of the A ring is critical for potency.

3.2. Effects of B ring modifications (ABI-II-2)

In general, compounds with modifications on the N-1 position in the B ring show decreased activity compared with their parental compounds (Table 1). Specifically, **3aa** (Table 1, 0.94 μM) had a 90-fold decrease in potency when compared with its parent compound **1a** (Fig. 3, 0.01 μM),[10] indicating that the large benzyl group was not well tolerated. **3ab** (Table 1, 0.03 μM) showed slightly decreased activity compared with the parent compound **1a** (Fig. 3, 0.01 μM),[10] which may imply that a smaller group is optimal. However, compound **3b** lost activity completely (Table 1, >10 μM) compared with its parent compound **1b** (Fig. 3, 0.03 μM),[10] suggesting that the binding mechanism of this compound is profoundly different than that of its congener, compound **3aa**. Compound **7b**, with a *para*-methoxy-phenylsulfonyl group on the N-1 position of the B

Table 1
In vitro growth inhibitory effects of ABI-II compounds on melanoma and prostate cancer.

Structure	ID	R^1	R^2	R^3	IC_{50} ± SEM (μM) (n = 4)					
					A375	WM164	LNCaP	PC-3	Du 145	PPC-1
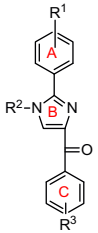	**2a**	4-Me	H	3,5-$(OMe)_2$,4-OH	0.11 ± 0.02	0.12 ± 0.02	0.13 ± 0.04	0.13 ± 0.08	0.17 ± 0.07	0.11 ± 0.02
	2c	4-Cl	H	3,5-$(OMe)_2$,4-OH	0.68 ± 0.15	0.50 ± 0.06	0.55 ± 0.01	0.30 ± 0.08	1.00 ± 0.21	0.58±0.02
	3aa	4-Me	Bn	3,4,5-$(OMe)_3$	1.06 ± 0.22	1.17 ± 0.35	0.68 ± 0.02	0.47 ± 0.04	1.50 ± 0.52	0.78 ± 0.01
	3ab	4-Me	Me	3,4,5-$(OMe)_3$	0.03 ± 0.01	0.04 ± 0.02	0.03 ± 0.01	0.04 ± 0.02	0.03 ± 0.01	0.03 ± 0.01
	3b	4-OMe	Me	4-F	>10	>10	>10	>10	>10	>10
	7b	4-$N(Me)_2$	(4-OMe)$PhSO_2$	4-F	0.10 ± 0.02	0.10 ± 0.01	0.07 ± 0.02	0.04 ± 0.01	0.13 ± 0.01	0.06 ± 0.01
	8a	4-Br	H	3,4,5-$(OMe)_3$	0.03 ± 0.01	0.04 ± 0.01	0.03 ± 0.01	0.04 ± 0.01	0.05±0.02	0.03 ± 0.01
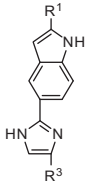	**21b**	3,4,5-$(OMe)_3$-PhCO		3,4,5-$(OMe)_3$-PhCO	1.80 ± 0.35	1.70 ± 0.20	1.07 ± 0.15	2.63 ± 0.58	5.92 ± 0.66	4.58 ± 0.63
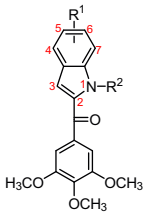	**11b**	6-F	$PhSO_2$	NA	>10	>10	>10	>10	>10	>10
	11c	6-OMe	$PhSO_2$	NA	8.22 ± 0.81	>10	>10	2.66 ± 0.53	>10	1.05 ± 0.07
	12a	6-Cl	H	NA	>10	>10	>10	>10	>10	>10
	12b	6-F	H	NA	>10	>10	>10	>10	>10	>10
	12c	6-OMe	H	NA	>10	>10	>10	>10	>10	>10
	12d	5-Cl	H	NA	1.47 ± 0.37	2.16 ± 0.26	>10	>10	>10	>10
	12e	6-Me	H	NA	>10	>10	>10	>10	>10	>10
	12f	5-F	H	NA	2.21 ± 0.16	2.26 ± 0.45	8.63 ± 0.59	9.16 ± 1.14	3.42 ± 0.17	1.00 ± 0.02
	12h	5-OMe	H	NA	0.03 ± 0.01	0.04 ± 0.01	0.05 ± 0.02	0.04 ± 0.01	0.08 ± 0.01	0.05 ± 0.01
	13aa	6-Cl	Me	NA	6.65 ± 0.33	8.08 ± 1.21	1.04 ± 0.25	3.76 ± 0.83	>10	4.33 ± 0.72
	13ab	6-Cl	Bn	NA	>10	>10	>10	>10	>10	>10
	13b	6-F	Me	NA	5.87 ± 0.24	7.50 ± 0.46	1.05 ± 0.09	>10	>10	8.30 ± 1.32
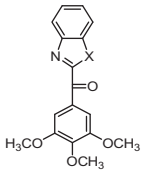	**12g**	X = NH			>10	>10	>10	>10	>10	>10
	15a	X = S			>10	>10	>10	>10	>10	>10
	15b	X = O			>10	>10	>10	>10	>10	>10
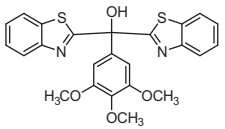	**15aa**	NA			>10	>10	>10	>10	>10	>10
Colchicine					0.02 ± 0.01	00.03 ± 0.02	0.02 ± 0.01	0.01 ± 0.01	00.01 ± 0.01	0.02 ± 0.01

NA—not applicable.

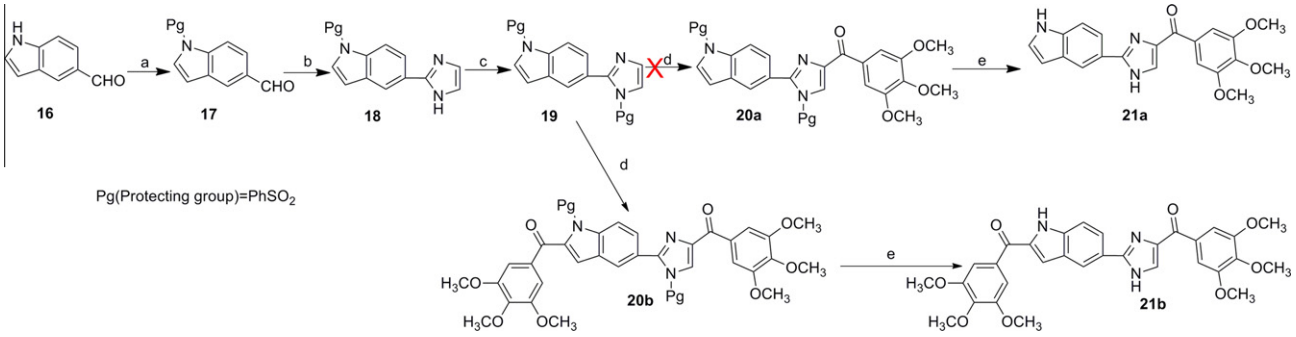

Scheme 4. Reagents and conditions: (a) (1) KOH, ethanol; (2) $PhSO_2Cl$, acetone; (b) NH_4OH, glyoxal, ethanol, rt; (c) NaH, $PhSO_2Cl$, THF, 0 °C–rt; (d) *t*-BuLi (1.7 M in pentane), benzoyl chloride, THF, −78 °C; (e) NaOH, ethanol, H_2O, reflux.

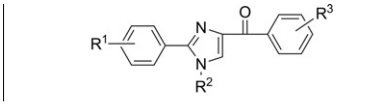

Figure 3. Antiproliferative activities of ABI-I analogs.[10]

ring, showed comparable activity (Table 1, 0.08 μM) to the parent compound **7c** (Fig. 3, 0.06 μM),[10] which has a phenylsulfonyl group on the N-1 position of the B ring, indicating that electronic effect provided by the substitution group on the N-1 position of the B ring was not significant in the binding interaction with the target.

3.3. Effects of C ring modifications (ABI-II-3)

For the C ring modification, the *para*-hydroxy compound was designed to test the pharmacologic activity of this potential metabolite, as the 3,4,5-trimethoxy was found to be labile to demethylation under both in vitro (in the presence of liver microsomes) and in vivo conditions.[17] Unfortunately, this modification led to a compound with a 10- to 20-fold decrease in activity when compared with **2a** (0.13 μM), **2c** (0.62 μM) (Table 1), and their parent compounds **1a** (Fig. 3, 0.01 μM) and **1c** (Fig. 3, 0.03 μM).[10]

3.4. Effects of fused A and B rings (ABI-II-4)

Surprisingly, for the compounds with fused A and B rings, most were inactive (Table 1). Some of them showed moderate activity with IC_{50} values in the micromolar range as exemplified by compounds **13aa**, **13b**, **12d**, and **12f** (1–10 μM). When comparing **13aa** (N-methylated-**12a**, 5.6 μM), **13ab** (N-benzylated-**12a**, >10 μM), and **12a** (>10 μM), **13aa** was the best in this series (6-Cl-indole analogues), which may suggest that the methyl group on the indole N-1 position of **13aa** is favorable for activity while a benzyl group on the N-1 position of **13ab** diminishes activity. This finding was further confirmed by comparing **13b** (methylated-**12b**, 1–10 μM) and **12b** (>10 μM). Compound **12f** (4.4 μM), with a 5-F on the indole ring, may have a more favorable binding mode over its 6-F counterpart compound **12b** (>10 μM), which was further verified by comparing 5-Cl compound **12d** (1.4 and 2.1 μM in A375 and WM164, respectively) and its 6-Cl counterpart compound **12a** (>10 μM) as well as the comparison between 5-OCH_3 compound **12h** (0.05 μM) and its 6-OCH_3 counterpart compound **12c** (>10 μM). The substantial differences in the activity of 5- and 6-substituted compounds suggest that the substitution on position 5 may have a favorable binding interaction with tubulin over position 6. This is consistent with the literature in which the 5-substitued analogues demonstrated excellent activity,[14] while 6-subsitituted compounds were generally inactive. Other ring systems such as benzoxazole (**15b**), benzimidazole (**12g**), and benzothiazole (**15a**, **15aa**) led to inactive compounds (>10 μM).

3.5. Effects of 3ab (an ABI-II-2 compound) and 8a (an ABI-II-1 compound) on multidrug resistant cell lines

Pgp-mediated drug efflux represents a major drug resistant mechanism for tumor cells to evade the buildup of effective intracellular drug concentrations. The clinical use of important tubulin-targeting drugs, such as paclitaxel and vinblastine, suffers from multidrug resistance, with Pgp efflux as the major mechanism.[18–20] Tubulin polymerization inhibitors that can effectively circumvent drug resistance mechanisms could significantly improve clinical efficacy. Previously, we showed that ABI-I analogs can overcome the Pgp-mediated mechanism.[10] We hypothesized that ABI-II analogs derived from ABI-I retain this property and may overcome additional paclitaxel resistance mechanisms. To test this hypothesis, we selected the most active compounds, **3ab** and **8a**, and tested their activity in two separate studies. In both studies, we included paclitaxel for comparison.

In the first study, we tested the activity of **3ab** and **8a** in a Pgp-overexpressed cancer cell line (MDA-MB-435/LCC6MDR1) and its parental, nonresistant cell line (MDA-MB-435). MDA-MB-435 was originally designated as a breast cancer cell line, but later it was shown to have originated from the human M14 melanoma cell line.[21] This pair of cell lines has been well validated and widely used to assess abilities of drugs overcoming Pgp-mediated multidrug resistance.[22] As can be seen from Table 2, compounds **3ab** and **8a** demonstrated better drug resistance indices ($R = 0.8$ and 0.9, respectively) than does paclitaxel ($R = 29$).

Having confirmed that ABI-II analogs retain the activity against Pgp-mediated drug resistance, we performed a second experiment to test whether these compounds could be effective against other paclitaxel-resistance mechanisms. We obtained two pairs of paclitaxel-resistant human prostate cancer cell lines (PC-3-TxR and DU-145-TxR) and their sensitive parental cell lines from Dr. Evan Keller's lab at the University of Michigan.[23] Subsequent analyses indicated that, in addition to Pgp overexpression, more than 200 genes are upregulated in PC-3-TxR and DU145-TxR cells, which may represent additional paclitaxel drug resistance mechanisms.[23] As shown in Table 2, the drug resistant indices increased substantially for paclitaxel in these cell lines ($R = 437$ and 1300 for PC-3-TxR and DU145-TxR, respectively) compared with that in MDA-MB-435/LCC6MDR1 ($R = 29$), suggesting that additional paclitaxel drug resistant mechanisms may play a role. In contrast, both **3ab** and **8a** ($R \approx 1$) retained their efficacy against paclitaxel-resistant cancer cell lines. These results suggest that ABI analogs

Table 2
Antiproliferative activity of ABI-II analogs on multidrug resistant cell lines

ID	IC_{50} ± SEM (nM) (n = 4)						
	MDA-MB-435	MDA-MB-435/LCC6MDR1	PC-3	PC-3-TxR	Du145	DU145-TxR	Resistance index (R)*
3ab	83 ± 22	67 ± 13	21 ± 1	19 ± 1	53 ± 1	52 ± 3	0.8/0.9/1.0
8a	86 ± 11	79 ± 20	18 ± 3	16 ± 4	49 ± 3	54 ± 3	0.9/0.9/1.1
Paclitaxel	16 ± 4	465 ± 53	0.43 ± 0.04	188 ± 22	2.3 ± 0.1	>3000	29/437/1300

* The three different numbers in each cell of this column represent the resistance indices of MDA-MB-435/LCC6MDR1, PC-3-TxR, and Du145-TxR, respectively; Resistance indices (R) were calculated by dividing IC_{50} values on multidrug resistant cell lines MDA-MB-435/LCC6MDR1, PC-3-TxR, and DU145-TxR by IC_{50} values on the matching sensitive parental cell line MDA-MB-435, PC-3, and Du145, respectively. The larger the R value, the more resistant the drug.

may overcome paclitaxel-resistance mechanisms, in addition to the well known Pgp-mediated mechanism.

Although paclitaxel demonstrated excellent activity in nonresistant cancer cell lines (0.4–17 nM), it was significantly less potent in the MDR cancer cell lines (>400 nM). In contrast, **3ab** and **8a** had essentially equivalent potency on both resistant (50–80 nM) and nonresistant cancer cell lines (50–80 nM). These results are consistent with a recent report in which a structurally similar compound with the same mechanism of action was effective against cancer cells that overexpress Pgp, multidrug resistance-associated proteins (MRP), and breast cancer resistance protein (BCRP).[24] Collectively, these studies indicate that **3ab** and **8a** could effectively overcome the multidrug resistance and may provide therapeutic advantages over paclitaxel.

4. In vitro metabolic stability studies

4.1. Hepatic stability

In our previous study, we found that compound **1a**, the parent compound of **3ab**, was highly potent in vitro (Fig. 3, 0.01 μM); compound **1a** showed improved oral bioavailability, presumably due to its increased aqueous solubility over the SMART compounds.[12] However, further improvement of its PK properties was needed because of high clearance. Methylation of an imidazole ring is one potential strategy that can increase oral bioavailability without impacting potency;[25] compound **3ab** was designed in this manner. Prior to in vivo PK studies, we performed in vitro metabolic stability studies with **3ab** and its parent compound, **1a**.

Both **3ab** and **1a** were examined for metabolic stability in vitro by using liver microsomes obtained from human, rat, mouse, and dog (Fig. 4). Both of the compounds showed species differences in their metabolic stability. Surprisingly, compound **1a** was superior to **3ab** with respect to metabolic stability. In human liver microsomes, **3ab** and **1a** demonstrated similar half-lives, while in the presence of rat and mice microsome, **3ab** showed a shorter half-life (5 and 10 min in mouse and rat, respectively) than did **1a** (12 and 20 min in mouse and rat, respectively). In dog, compound **3ab** had a slightly longer half-life than that of compound **1a**. The results indicated that the methyl group on the imidazole ring is not beneficial for improving metabolic stability, especially in mice and rats. Therefore, further in vivo pharmacokinetic studies were not performed for **3ab**.

4.2. Metabolic pathway of compound 3ab

Liquid chromatography–tandem mass spectrometry was used to identify the metabolites of **3ab** after incubating with liver microsomes from the four species (Fig. 5). Hydroxylation on the *para*-methyl of the A ring was a major metabolic pathway of **3ab** in all species. This finding was consistent with our previous study.[12] O-Demethylation was a minor metabolic pathway, but it was found in each species. In mouse and rat, N-demethylation represented the major pathway that correlated well with the shorter half-life of **3ab** in comparison with that of **1a** in the presence of mouse and rat live microsomes (Fig. 4). Ketone reduction was only detected in human liver microsomes, suggesting that preclinical studies may not completely reflect human metabolism. However, we did not exhaustively test for the presence of the ketone reduced metabolite in liver microsomes from mice, rats and dogs. These metabolic studies revealed the labile sites of the ABI analogs in different species and can be used to direct further modifications of the ABI scaffold to obtain novel compounds with improved PK and drug-like properties.

5. Tubulin polymerization assay on ABI-II compounds

Based on their high structure similarity, we hypothesized that ABI-II compounds exert their effect through the inhibition of tubulin polymerization, similar to that of ABI-I compounds.[10] We therefore performed experiments to test the inhibition of tubulin polymerization by ABI-II analogs. Bovine brain tubulin (>97% pure) was incubated with three potent ABI-II compounds, **3aa**, **3ab**, and **8a**, along with colchicine as a positive control, at concentrations of 5, 10, 20 μM, respectively. All tested ABI-II compounds inhibit tubulin polymerization in a dose-dependent manner (Fig. 6). Complete inhibition of tubulin polymerization was observed after 15 min of treatment with **3ab** (Fig. 6A) at 20 μM, colchicine (Fig. 6D) at 20 μM, or compound **8a** at both 10 and 20 μM (Fig. 6B). In contrast, compound **3aa** (Fig. 6C) inhibited only 40% of tubulin polymerization at the highest concentration of 20 μM. These results are consistent with the relative antiproliferative potency for compound **3aa** (IC_{50} = 0.94 μM) and those of **3ab** (IC_{50} = 0.03 μM) and **8a** (IC_{50} = 0.04 μM).

6. Molecular modeling studies on 3aa and 3ab

Since ABI-I compounds inhibit tubulin polymerization by binding to the colchicine site in tubulin,[10] based on the tubulin polymerization studies described above and the high structural similarity between ABI-I and ABI-II analogs, we believe that ABI-II compounds also bind to the colchicine binding site in tubulin. Therefore, we examined the potential binding modes of ABI-II and their interactions with the receptor at the colchicine site in the tubulin dimer by using Schrodinger 2011 molecular modeling suite (Schrodinger, Inc., New York, NY). We selected the crystal structure of TN16-tubulin complex for these studies because the structure of TN-16 (Fig. 1) is the closest to the structure of **3ab**.[26] Results for docking of **3ab** and **3aa** illustrate the binding mode of ABI-II analogs (Fig. 7). Figure 7A shows the overview of the compound binding in relation to the α/β tubulin dimer, and Figure 7B shows the details of the binding pocket, which is framed by dotted surface. The structures of **3ab** (green tube model) and TN16 (red wire model) overlap very well in the colchicine binding pocket. The smaller 4-methylphenyl group (A ring) of **3ab** is inserted deeply into the β-subunit, while its larger end, the 3,4,5-trimethoxybenzoyl group (C ring), extends toward the α/β interface.

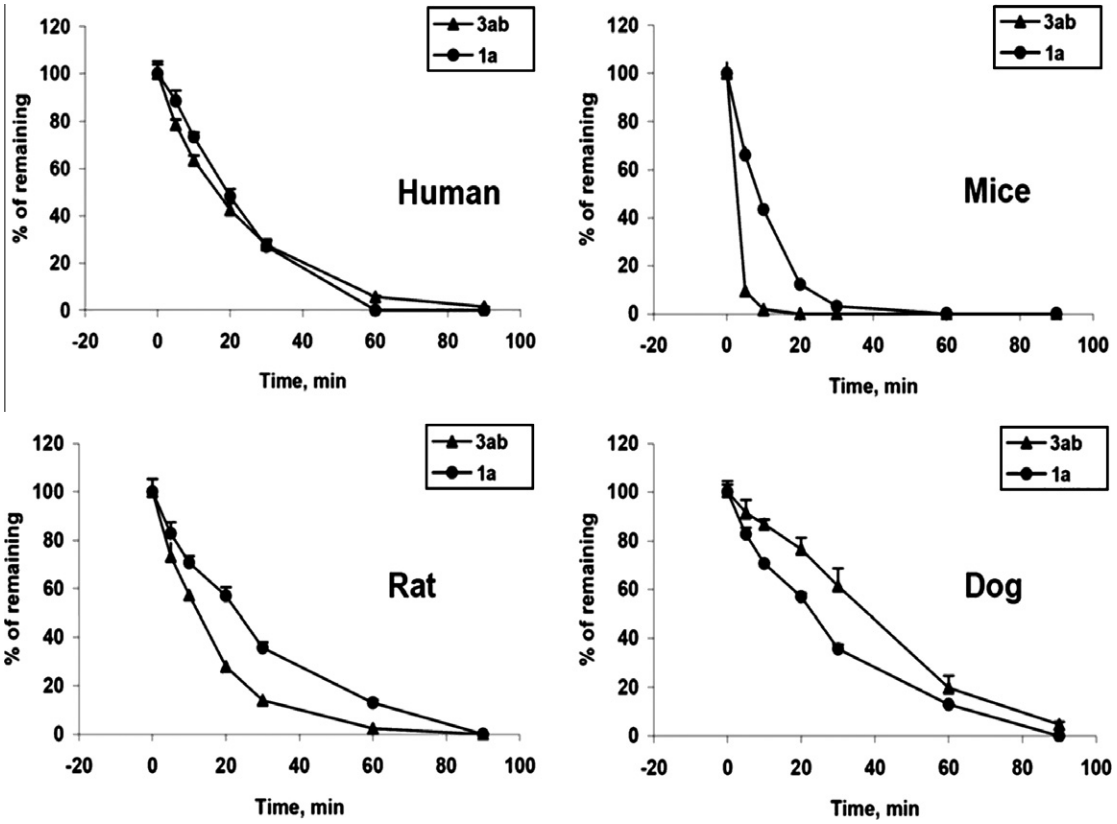

Figure 4. In vitro metabolic profiles of **3ab** and **1a**.

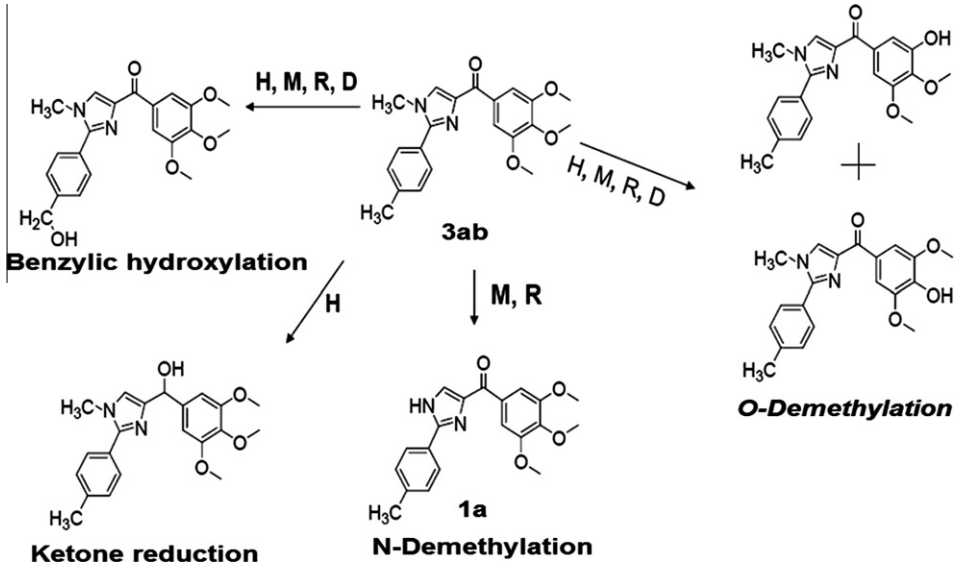

Figure 5. In vitro metabolism of **3ab** and **1a**. H, M, R, and D indicate human, mouse, rat, and dog microsomes, respectively. Bold denotes major pathway.

Interestingly, when the B ring N-substituent switches from a methyl moiety in **3ab** to a benzyl group in **3aa**, the corresponding binding mode turns upside down. The bulky side of **3aa**, which consists of the B ring *N*-benzyl moiety and A ring 4-methylphenyl group, is forced to occupy the wide upper location of the pocket. Additionally, the C ring of **3aa** shifts up from the narrow bottom of the lower pocket region. As a result, the hydrophobic interactions and likely formation of hydrogen bonds between the ligand and residues of tubulin, such as TYR202 in S6, LEU242 in H7, and MET259 in H8, may have been reduced greatly and thus lead to the decreased in vitro activity from **3ab** to **3aa**.

It is noteworthy to mention that the best binding poses suggested by molecular modeling for the colchicine binding site seem to be strongly influenced by the choice of the starting ligand–tubulin complex. We previously used the DAMA-colchicine in the tubulin complex for studying potential binding pose of ABI-I analogs.[10] When we used a different ligand–tubulin complex in which the ligand TN-16 (Fig. 1) is more similar to ABI analogs, we obtained the

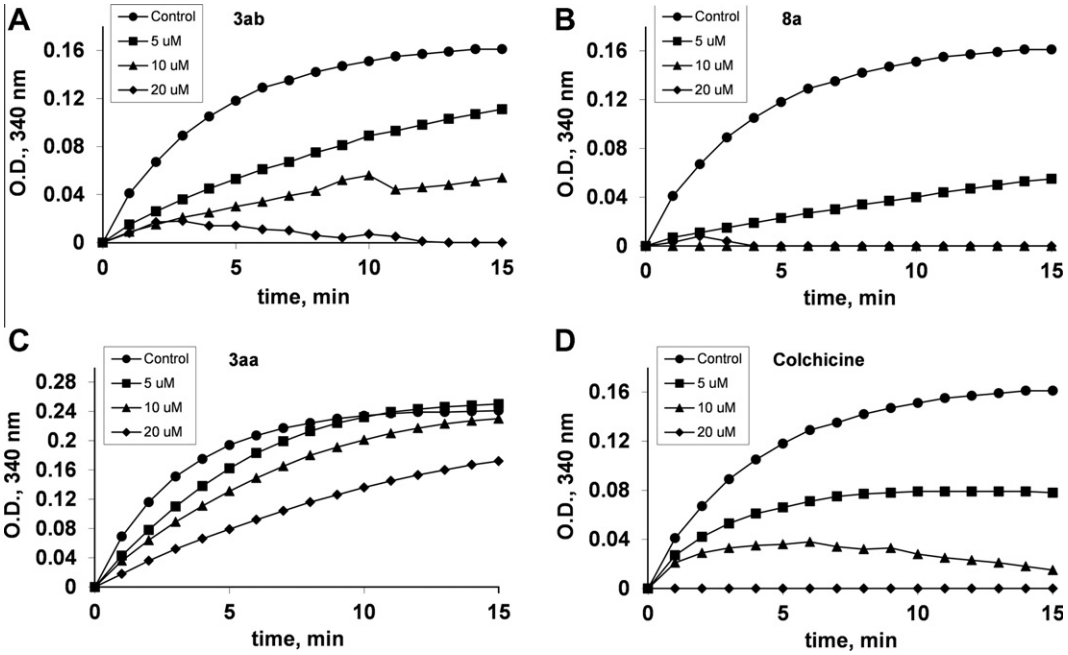

Figure 6. Effect of ABI-II compounds on tubulin polymerization in vitro. Tubulin (0.4 mg/assay) was exposed to 5, 10, 20 μM ABI-II compounds (vehicle control, 5% DMSO) **3ab** (panel A), **8a** (panel B), **3aa** (panel C) or colchicine (positive control, panel D). Absorbance at 340 nm was monitored at 37 °C every minute for 15 min.

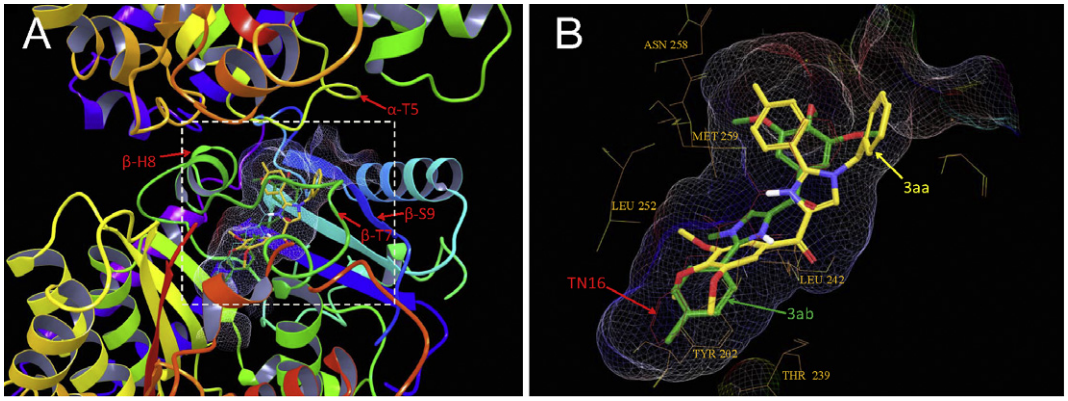

Figure 7. Binding modes of **3aa** and **3ab** in the colchicine binding site of tubulin.

alternative best binding poses described above. The major difference is that the overall ligand geometry is more linear and penetrates deeper into the binding pocket of the β-tubulin monomer (Fig. 7). Because of the difficulty and complexity of tubulin crystal structures, all existing tubulin complexes have very poor resolution (RMS >3 Å). Both of the binding poses are theoretically possible, but the true binding pose can be obtained only by solving ABI-tubulin crystal structures in the future.

7. Conclusions

In summary, we synthesized ABI-II compounds and performed extensive SAR studies. Although most of the ABI-II compounds are less potent than are ABI-I compounds, they provide deep insight into the pharmacophore of ABI analogues. The in vitro metabolic studies on **3ab** showed that N-methylation on the imidazole ring is not beneficial for improving metabolic stability; however, a better pharmacokinetic profile may be achieved upon appropriate modification on the imidazole NH, thus providing a better opportunity for the ABI analogs to be developed into a more drug-like anticancer agent. Therefore, the metabolic pathway of **3ab** not only revealed the labile sites of ABI analogs but also laid the foundation for further modification of the ABI analogs toward a more druggable direction.

8. Experimental section

8.1. General

All reagents were purchased from Sigma–Aldrich Chemical Co. (St. Louis, MO), Fisher Scientific (Pittsburgh, PA), Alfa Aesar (Ward Hill, MA), and AK Scientific (Mountain View, CA) and were used without further purification. The solvents for moisture-sensitive reactions were freshly distilled, and the reactions were carried out in an argon atmosphere. Routine thin-layer chromatography (TLC) was performed on aluminum-backed Uniplates (Analtech, Newark, DE). Melting points were measured with the Fisher-Johns melting point apparatus (uncorrected). Nuclear magnetic resonance spectra were obtained on a Varian Inova-500 spectrometer (Santa Clara CA) or a Bruker AX 300 (Billerica, MA) spectrometer.

Chemical shifts are reported as parts per million (ppm) relative to TMS in $CDCl_3$. Mass spectra were collected on a Bruker ESQUIRE electrospray/ion trap instrument in positive and negative ion modes. The purity of the final compounds was examined via reverse phase high performance liquid chromatography RP-HPLC on a Waters 2695 HPLC system equipped with a photodiode array detector (Milford, MA). Two RP-HPLC methods were conducted using a Supelco Ascentis™ 5 μM RP-Amide column (250 × 4.6 mm) from Sigma–Aldrich (St. Louis, Mo) at ambient temperature, and a flow rate of 0.7 mL/min. HPLC1: Gradient: Solvent A (water) and Solvent B (methanol): 0–15 min 40–100% B (linear gradient), 15–25 min 100% B. HPLC2: Gradient: Solvent A (water) and Solvent B (methanol): 0–5 min 10–40% B (linear gradient), 5–15 min 40–100% B, 15–30 min 100% B. UV detection at 254 nm. Purity of the compounds was established by careful integration of areas for all peaks detected and is reported for each compound in Section 8.2.

8.2. General procedure for the synthesis of (2-aryl-1*H*-imidazol-4-yl)methanone (2a, 2c, 3aa, 3ab, 3b) and (1-substituted-indol-2-yl)(3,4,5-trimethoxyphenyl)methanone (13aa, 13ab, 13b)

8.2.1. Compounds 2a and 2c

To a solution of ABI-I (**1a** and **1c**, 200–210 mg, 0.57 mmol) in THF (20 mL) was added aluminum chloride (758 mg, 5.7 mmol). The reaction mixture was stirred overnight. Water was added followed by extraction with ethyl acetate (150 ml). The organic layer was dried over magnesium sulfate and concentrated. The residue was subjected to flash column chromatography (hexane/ethyl acetate, 1:1) to give a white-yellowish solid. Yield: 60–80%.

8.2.2. Compounds 3aa, 3ab, 3b, 13aa, 13ab, 13b

To a solution of ABI-I (**1a** and **1b**) or (1*H*-indol-2-yl)(3,4,5-trimethoxyphenyl)methanone **(12a, 12b)** (100–150 mg, 0.4 mmol) in THF (10 mL) in ice-bath was added sodium hydride (60% dispersion in mineral oil, 28 mg, 0.60 mmol) followed by adding methyl iodide (85 mg, 0.60 mmol) (for **3ab, 3b, 13aa, 13b**) or benzyl bromide (102 mg, 0.60 mmol) (for **3aa, 13ab**). The resulting reaction mixture was stirred for 5 h under reflux condition. After dilution by 50 ml of saturated $NaHCO_3$ solution (aqueous), the reaction mixture was extracted by ethyl acetate (100 ml). The organic layer was dried over magnesium sulfate and concentrated. The residue was purified by flash column chromatography (hexane/ethyl acetate, 2:1) to give a white solid. Yield: 50–98%.

8.3. General procedure the synthesis of 2-aryl-1*H*-imidazole (18, 5a and 5b)

To a solution of appropriate benzaldehyde (**17**, **4a**, and **4b**, 14–28 g, 100 mmol) in ethanol (400 ml) at 0 °C was added a solution of 40% oxalaldehyde in water (16 g, 110 mmol) and a solution of 29% ammonium hydroxide in water (120 g, 1000 mmol). After stirring for 2–3 days at room temperature, the reaction mixture was concentrated, and the residue was subjected to flash column chromatography with dichloromethane as eluent to yield the titled compound as a yellow powder. Yield: 10–30%.

8.4. General procedure for the synthesis of (2-aryl-1*H*-imidazol-4-yl)methanone (8a)

To a solution of aryl (2-aryl-1-(phenylsulfonyl)-1*H*-imidazol-4-yl) methanone (**7a**, 1.1 g, 2.0 mmol) in THF (25.0 ml) was added 1.0 M tetrabutyl ammonium fluoride (4 mL, 4.0 mmol) and stirred overnight. The reaction mixture was diluted by 60 ml of saturated $NaHCO_3$ solution (aqueous) and extracted by ethyl acetate (150 ml). The organic layer was dried over magnesium sulfate and concentrated. The residue was purified by flash column chromatography (hexane/ethyl acetate, 4:1) or recrystallized from water and methanol to give a white solid. Yield: 80%.

8.5. General procedure for the synthesis of 2-aryl-1-(phenylsulfonyl)-1*H*-imidazole (6a–b, 19), 1-(phenylsulfonyl)-1*H*-indole (10a–f, 10h), and 1-(phenylsulfonyl)-1*H*-benzo[*d*]imidazole (10g)

To a solution of imidazoles (**5a, 5b, 18**), indoles (**9a–f, 9h**), or benzimidazole (**9g**) (1.3–3.5 g, 10 mmol) in anhydrous THF (200 ml) at 0 °C was added sodium hydride (60% dispersion in mineral oil, 48 mg, 12 mmol) and stirred for 20 min. 4-Methoxybenzenesulfonyl chloride (2.5 g, 12 mmol) (for **6b**) or benzenesulfonyl chloride (2.1 g, 12 mmol) (for others) was added, and the reaction mixture was stirred overnight. After dilution by 200 ml of saturated $NaHCO_3$ solution (aqueous), the reaction mixture was extracted by ethyl acetate (600 ml). The organic layer was dried over magnesium sulfate and concentrated. The residue was purified by flash column chromatography (hexane/ethyl acetate, 2:1) to give a pale solid. Yield: 40–95%.

8.6. General procedure for the synthesis of aryl (2-aryl-1-(phenylsulfonyl)-1*H*-imidazol-4-yl)methanone (7a–b, 20b), (1-(phenylsulfonyl)-1*H*-indol-2-yl)(3,4,5-trimethoxyphenyl)-methanone (11a–f, 11h), (1-(phenylsulfonyl)-1*H*-benzo[*d*]-imidazol-2-yl)(3,4,5-trimethoxyphenyl)methanone (11g), benzo[*d*]thiazol-2-yl(3,4,5-trimethoxyphenyl)methanone (15a), and benzo[*d*]oxazol-2-yl(3,4,5-trimethoxyphenyl)-methanone (15b)

To a solution of 2-aryl-1-(phenylsulfonyl)-1*H*-imidazole (**6a–b**, **19**), 1-(phenylsulfonyl)-1*H*-indole **(10a–f, 10h)**, or 1-(phenylsulfonyl)-1*H*-benzo[*d*]imidazole **(10g)** or benzothiazole (**14a**), benzoxazole (**14b**) (1.6–2.3 g, 5.0 mmol) in anhydrous THF (30 ml) at −78 °C was added 1.7 M *tert*-butyllithium in pentane (3.5 mL, 6.0 mmol) and stirred for 10 min. 3,4,5-Trimethoxybenzoyl chloride (1.4 g, 6.0 mmol) was added at −78 °C and stirred overnight. The reaction mixture was diluted with 100 ml of saturated $NaHCO_3$ solution (aqueous) and extracted by ethyl acetate (300 ml). The organic layer was dried over magnesium sulfate and concentrated. The residue was purified by flash column chromatography (hexane/ethyl acetate, 3:1) to give a white solid. Yield: 5–45%.

8.7. General procedure for the synthesis of (1*H*-benzo[*d*]-imidazol-2-yl)(3,4,5-trimethoxyphenyl)methanone (12g), (1*H*-indol-2-yl)(3,4,5-trimethoxyphenyl)methanone (12a–f, 12h), and (2-aryl-1*H*-imidazol-4-yl)methanone (21b)

To a solution of (1-(phenylsulfonyl)-1*H*-indol-2-yl)(3,4,5-trimethoxyphenyl)methanone **(11a–f, 11h)**, (1-(phenylsulfonyl)-1*H*-benzo[*d*]imidazol-2-yl)(3,4,5-trimethoxyphenyl)methanone **(11g)**, or (1-(phenylsulfonyl)-2-(1-(phenylsulfonyl)-2-(3,4,5-trimethoxybenzoyl)-1*H*-indol-5-yl)-1*H*-imidazol-4-yl)(3,4,5-trimethoxyphenyl)methanone **(20b)** (450–850 mg, 1.0 mmol) in ethanol (20 ml) was added sodium hydroxide (400 mg, 10 mmol) and stirred overnight in darkness. The reaction mixture was diluted by 50 ml of water and extracted by ethyl acetate (250 ml). The organic layer was dried over magnesium sulfate and concentrated. The residue was purified by flash column chromatography (hexane/ethyl acetate 3:1) or recrystallized from water and methanol to give a white solid. Yield: 30–95%.

8.8. Synthesis of 1-(phenylsulfonyl)-1*H*-indole-3-carboxaldehyde (17)

To a solution of indole-3-carboxaldehyde (**16**, 28.5 g, 100 mmol) in ethanol (500 mL) at room temperature was added potassium hydroxide (6.2 g, 110 mmol); the mixture was stirred until total solubilization. The ethanol was completely removed in a vacuum and acetone (250 mL) was added followed by benzenesulfonyl chloride (19.4 g, 110 mmol). The precipitate was filtered off, and the filtrate was concentrated and recrystallized from methanol to give a white solid. Yield: 40%.

8.9. (4-Hydroxy-3,5-dimethoxyphenyl)(2-(*p*-tolyl)-1*H*-imidazol-4-yl)methanone (2a)

Yield: 56.8%; mp 220–222 °C. ^{1}H NMR ($CDCl_3$, 500 MHz) δ 8.02 (d, J = 8.0 Hz, 2H), 7.91 (s, 1H), 7.39 (s, 2H), 7.28 (d, J = 7.5 Hz, 2H), 4.00 (s, 6H), 2.44 (s, 3H). MS (ESI) calcd for $C_{19}H_{18}FN_2O_4$ 338.1, found 339.1 $[M+H]^+$. HPLC1: t_R 3.91 min, purity 96.5%.

8.10. (2-(4-Chlorophenyl)-1*H*-imidazol-4-yl)(4-hydroxy-3,5-dimethoxyphenyl)methanone (2c)

Yield: 80.2%; mp 216–218 °C. ^{1}H NMR (CD_3OD, 500 MHz) δ 8.06 (d, J = 8.5 Hz, 2H), 7.99 (s, 1H), 7.61 (d, J = 8.0 Hz, 2H), 7.52 (s, 2H), 4.01 (s, 6H). MS (ESI) calcd for $C_{18}H_{15}ClN_2O_4$ 358.1, found 359.1 $[M+H]^+$. HPLC2: t_R 4.12 min, purity >99%.

8.11. (1-Benzyl-2-(*p*-tolyl)-1*H*-imidazol-4-yl)(3,4,5-trimethoxyphenyl)methanone (3aa)

Yield: 92.8%; mp 135–137 °C. ^{1}H NMR ($CDCl_3$, 500 MHz) δ 7.81 (s, 1H), 7.80 (d, J = 6.5 Hz, 2H), 7.58 (d, J = 8.0 Hz, 2H), 7.41–7.45 (m, 3H), 7.31–7.33 (m, 2H), 7.20 (d, J = 7.0 Hz, 2H), 5.33 (s, 2H), 3.99 (s, 3H), 3.98 (s, 6H), 2.47 (s, 3H). MS (ESI) calcd for $C_{27}H_{26}N_2O_4$ 442.2, found 443.1 $[M+H]^+$. HPLC1: t_R 4.28 min, purity >99%.

8.12. Methyl-2-(*p*-tolyl)-1*H*-imidazol-4-yl)(3,4,5-trimethoxyphenyl)methanone (3ab)

Yield: 87.4%; mp 110–112 °C. ^{1}H NMR ($CDCl_3$, 500 MHz) δ 7.87 (s, 2H), 7.86 (d, J = 8.0 Hz, 1H), 7.65 (d, J = 10 Hz, 2H), 7.37 (d, J = 10 Hz, 2H), 4.01 (s, 6H), 4.00 (s, 3H), 3.90 (s, 3H), 2.53 (s, 3H). MS (ESI) calcd for $C_{21}H_{22}N_2O_4$ 366.2, found 367.2 $[M+H]^+$. HPLC1: t_R 4.23 min, purity >99%.

8.13. (4-Fluorophenyl)(2-(4-methoxyphenyl)-1-methyl-1*H*-imidazol-4-yl)methanone (3b)

Yield: 90.2%; mp 148–150 °C. ^{1}H NMR ($CDCl_3$, 500 MHz) δ 8.45 (q, J = 8.5 Hz, 5.5 Hz, 2H), 7.79 (s, 1H), 7.63 (d, J = 8.5 Hz, 2H), 7.16 (t, J = 8.5 Hz, 2H), 7.03 (d, J = 9.0 Hz, 2H), 3.89 (s, 3H), 3.82 (s, 3H). MS (ESI) calcd for $C_{18}H_{15}FN_2O_2$ 310.1, found 311.0 $[M+H]^+$. HPLC2: t_R 4.01 min, purity 97.6%.

8.14. 2-(4-Bromophenyl)-1*H*-imidazole (5a)

Yield: 19.5%. ^{1}H NMR ($CDCl_3$, 300 MHz) δ 12.59 (s, 1H), 7.87 (d, J = 8.1 Hz, 2H), 7.64 (d, J = 8.1 Hz, 2H), 7.27 (s, 1H), 7.04 (s, 1H). MS (ESI) calcd for $C_9H_7BrN_2$ 222.0, found 222.8 $[M+H]^+$.

8.15. 4-(1*H*-Imidazol-2-yl)-*N*,*N*-dimethylaniline (5b)

Yield: 16.9%. ^{1}H NMR (300 MHz, $CDCl_3$) δ 7.70 (dd, J = 7.0 Hz, 2.0 Hz, 2H), 7.10 (s, 2H), 6.75 (dd, J = 9.0 Hz, 2.0 Hz, 2H), 3.02 (s, 6H). MS (ESI): calcd for $C_{11}H_{13}N_3$, 187.1, found 187.9 $[M+H]^+$, 185.8 $[M-H]^-$.

8.16. 2-(4-Bromophenyl)-1-(phenylsulfonyl)-1*H*-imidazole (6a)

Yield: 61.2%. ^{1}H NMR ($CDCl_3$, 500 MHz) δ 7.71 (d, J = 2.0 Hz, 1H), 7.64 (t, J = 7.0 Hz, 1H), 7.57 (d, J = 9.0 Hz, 2H), 7.49 (d, J = 7.0 Hz, 2H), 7.45 (t, J = 9.0 Hz, 2H), 7.34 (d, J = 8.5 Hz, 2H), 7.18 (d, J = 1.5 Hz, 1H). MS (ESI) calcd for $C_{15}H_{11}BrN_2O_2S$ 362.0, found 363.0 $[M+H]^+$.

8.17. 4-(1-((4-Methoxyphenyl)sulfonyl)-1*H*-imidazol-2-yl)-*N*,*N*-dimethylaniline (6b)

Yield: 61.5%. ^{1}H NMR (500 MHz, $CDCl_3$) δ 7.58 (d, J = 1.5 Hz, 1H), 7.36 (t, J = 8.43 Hz, 4H), 7.03–7.09 (m, 1H), 6.80 (d, J = 9.0 Hz, 2H), 6.69 (d, J = 8.8 Hz, 2H), 3.84 (s, 3H), 3.05 (s, 6H). MS (ESI): calcd for $C_{18}H_{19}N_3O_3S$, 357.1, found 358.2 $[M+H]^+$.

8.18. (2-(4-Bromophenyl)-1-(phenylsulfonyl)-1*H*-imidazol-4-yl)(3,4,5-trimethoxyphenyl)methanone (7a)

Yield: 32.6% ^{1}H NMR ($CDCl_3$, 500 MHz) δ 8.06 (d, J = 8.0 Hz, 2H), 7.88 (d, J = 8.5 Hz, 1H), 7.77 (t, J = 7.0 Hz, 1H), 7.54–7.63 (m, 4H), 7.31–7.36 (m, 4H), 4.04 (s, 3H), 4.01 (s, 6H). MS (ESI) calcd for $C_{25}H_{21}BrN_2O_6S$ 556.0, found 557.0 $[M+H]^+$.

8.19. (2-(4-(Dimethylamino)phenyl)-1-((4-methoxyphenyl)sulfonyl)-1*H*-imidazol-4-yl)(4-fluorophenyl)methanone (7b)

Yield: 34.1%; mp 147–149 °C. ^{1}H NMR ($CDCl_3$, 500 MHz) δ 8.07 (q, J = 8.5 Hz, 5.5 Hz, 2H), 7.78 (d, J = 9.0 Hz, 2H), 7.41 (d, J = 8.5 Hz, 2H), 7.39 (s, 1H), 7.23 (t, J = 8.5 Hz, 2H), 6.91 (d, J = 9.0 Hz, 2H), 6.68 (d, J = 9.0 Hz, 2H), 3.89 (s, 3H), 3.08 (s, 6H). MS (ESI) calcd for $C_{25}H_{22}FN_3O_4S$ 479.1, found 502.0 $[M+Na]^+$. HPLC2: t_R 18.0 min, purity >99%.

8.20. (2-(4-Bromophenyl)-1*H*-imidazol-4-yl)(3,4,5-trimethoxyphenyl)methanone (8a)

Yield: 25.6%; mp 190–192 °C. ^{1}H NMR ($CDCl_3$, 500 MHz) δ 7.99 (d, J = 8.5 Hz, 2H), 7.92 (s, 1H), 7.70 (d, J = 8.5 Hz, 2H), 7.32 (s, 2H), 4.03 (s, 3H), 4.00 (s, 6H). MS (ESI) calcd for $C_{19}H_{17}BrN_2O_4$ 416.0, found 417.0 $[M+H]^+$. HPLC2: t_R 4.24 min, purity 98.8%.

8.21. 6-Chloro-1-(phenylsulfonyl)-1*H*-indole (10a)

Yield: 82.3%. ^{1}H NMR (500 MHz, $CDCl_3$) δ 8.09 (s, 1H), 7.95 (d, J = 7.8 Hz, 2H), 7.59–7.66 (m, 2H), 7.46–7.58 (m, 3H), 7.24–7.30 (m, 1H), 6.70 (d, J = 3.7 Hz, 1H). MS (ESI) calcd for $C_{14}H_{10}ClNO_2S$ 291.0, found 314.0 $[M+Na]^+$.

8.22. 6-Fluoro-1-(phenylsulfonyl)-1*H*-indole (10b)

Yield: 92.5%. ^{1}H NMR (500 MHz, $CDCl_3$) δ 7.95 (d, J = 7.8 Hz, 2H), 7.80 (dd, J = 2.0, 9.6 Hz, 1H), 7.58–7.66 (m, 2H), 7.47–7.57 (m, 3H), 7.06 (dt, J = 2.44 Hz, 8.9 Hz, 1H), 6.70 (d, J = 3.6 Hz, 1H). MS (ESI) calcd for $C_{14}H_{10}FNO_2S$ 275.1, found 298.1 $[M+Na]^+$.

8.23. 6-Methoxy-1-(phenylsulfonyl)-1*H*-indole (10c)

Yield: 93.8%. ^{1}H NMR (500 MHz, $CDCl_3$) δ 7.93 (d, J = 9.0 Hz, 2H), 7.58–7.61 (m, 2H), 7.49–7.52 (m, 3H), 7.45 (d, J = 9.0 Hz, 1H), 6.93 (dd, J = 9.5 Hz, 2.0 Hz, 1H), 6.65 (d, J = 3.0 Hz, 1H), 3.94 (s, 3H). MS (ESI) calcd for $C_{15}H_{13}NO_3S$ 287.1, found 310.0 $[M+Na]^+$.

8.24. 5-Chloro-1-(phenylsulfonyl)-1*H*-indole (10d)

Yield: 96.3%. ^{1}H NMR (500 MHz, $CDCl_3$) δ 7.99 (d, J = 9.0 Hz, 1H), 7.92 (d, J = 7.8 Hz, 2H), 7.68–7.59 (m, 2H), 7.56 (d, J = 1.7 Hz, 1H), 7.47–7.55 (m, 2H), 7.31–7.36 (m, 1H), 6.67 (d, J = 3.4 Hz, 1H).

MS (ESI) calcd for $C_{14}H_{10}ClNO_2S$ 291.0, found 314.0 $[M+Na]^+$.

8.25. 6-Methyl-1-(phenylsulfonyl)-1*H*-indole (10e)

Yield: 95.1%. ^{1}H NMR (500 MHz, $CDCl_3$) δ 7.94 (d, J = 7.8 Hz, 2H), 7.88 (s, 1H), 7.57–7.63 (m, 1H), 7.56 (d, J = 3.7 Hz, 1H), 7.44–7.53 (m, 3H), 7.12 (d, J = 7.8 Hz, 1H), 6.68 (d, J = 3.7 Hz, 1H), 2.54 (s, 3H). MS (ESI) calcd for $C_{15}H_{13}NO_2S$ 271.1, found 294.0 $[M+Na]^+$.

8.26. 5-Fluoro-1-(phenylsulfonyl)-1*H*-indole (10f)

Yield: 88.6%. ^{1}H NMR (500 MHz, $CDCl_3$) δ 8.00 (dd, J = 4.4, 9.0 Hz, 1H), 7.92 (d, J = 7.6 Hz, 2H), 7.67 (d, J = 3.7 Hz, 1H), 7.62 (t, J = 7.4 Hz, 1H), 7.51 (t, J = 7.8 Hz, 2H), 7.24 (dd, J = 2.4, 8.8 Hz, 1H), 7.11 (dt, J = 2.4 Hz, 9.0 Hz, 1H), 6.69 (d, J = 3.7 Hz, 1H). MS (ESI) calcd for $C_{14}H_{10}FNO_2S$ 275.1, found 298.1 $[M+Na]^+$.

8.27. 1-(Phenylsulfonyl)-1*H*-benzo[*d*]imidazole (10g)

Yield: 99%. ^{1}H NMR (500 MHz, $CDCl_3$) δ 8.46 (s, 1H), 8.07 (d, J = 7.6 Hz, 2H), 7.94 (d, J = 8.3 Hz, 1H), 7.84 (d, J = 7.6 Hz, 1H), 7.70 (t, J = 7.6 Hz, 1H), 7.59 (t, J = 7.8 Hz, 2H), 7.40–7.51 (m, 2H). MS (ESI) calcd for $C_{13}H_{10}N_2O_2S$ 258.1, found 259.0 $[M+H]^+$.

8.28. 5-Methoxy-1-(phenylsulfonyl)-1*H*-indole (10h)

Yield: 92.6%. ^{1}H NMR (500 MHz, $CDCl_3$) δ 7.84–7.90 (m, 3H), 7.51–7.53 (m, 2H), 7.43 (t, J = 8.0 Hz, 2H), 6.98 (d, J = 2.0 Hz, 1H), 6.93 (dd, J = 9.0 Hz, 2.5 Hz, 1H), 6.60 (d, J = 3.5 Hz, 1H), 3.82 (s, 3H). MS (ESI) calcd for $C_{15}H_{13}NO_3S$ 287.1, found 310.0 $[M+Na]^+$.

8.29. (6-Chloro-1-(phenylsulfonyl)-1*H*-indol-2-yl)(3,4,5-trimethoxyphenyl)methanone (11a)

Yield: 34.7%. ^{1}H NMR (500 MHz, $CDCl_3$) δ 8.17–8.25 (m, 3H), 7.69–7.75 (m, 1H), 7.60–7.66 (m, 2H), 7.58 (d, J = 8.3 Hz, 1H), 7.37 (dd, J = 1.5 Hz, 8.3 Hz, 1H), 7.32 (d, J = 9.3 Hz, 2H), 6.96 (s, 1H), 4.02 (s, 3H), 3.95 (s, 6H). MS (ESI) calcd for $C_{24}H_{20}ClNO_6S$ 485.1, found 508.0 $[M+Na]^+$.

8.30. (6-Fluoro-1-(phenylsulfonyl)-1*H*-indol-2-yl)(3,4,5-trimethoxyphenyl)methanone (11b)

Yield: 34.7%; mp 171–173 °C. ^{1}H NMR (500 MHz, $CDCl_3$) δ 8.22 (d, J = 7.5 Hz, 2H), 7.93 (dd, J = 1.8 Hz, 9.8 Hz, 1H), 7.67–7.75 (m, 1H), 7.57–7.67 (m, 3H), 7.29–7.34 (s, 2H), 7.15 (dt, J = 2.20 Hz, 8.91 Hz, 1H), 6.98 (s, 1H), 4.02 (s, 3H), 3.95 (s, 6H). MS (ESI) calcd for $C_{24}H_{20}FNO_6S$ 469.1, found 492.0 $[M+Na]^+$. HPLC1: t_R 4.01 min, purity >99%.

8.31. (6-Methoxy-1-(phenylsulfonyl)-1*H*-indol-2-yl)(3,4,5-trimethoxyphenyl)methanone (11c)

Yield: 26.4%; mp 156–158 °C. ^{1}H NMR (500 MHz, $CDCl_3$) δ 8.18 (d, J = 7.8 Hz, 2H), 7.73 (s, 1H), 7.71–7.65 (m, 1H), 7.57–7.63 (m, 2H), 7.53 (d, J = 8.5 Hz, 1H), 7.32 (s, 2H), 7.01 (dd, J = 1.8 Hz, 8.7 Hz, 1H), 6.99 (s, 1H), 4.01 (s, J = 5.9 Hz, 6H), 3.95 (s, 6H). MS (ESI) calcd for $C_{25}H_{23}NO_7S$ 481.1, found 504.1 $[M+Na]^+$. HPLC1: t_R 3.99 min, purity 98.3%.

8.32. (6-Chloro-1-(phenylsulfonyl)-1*H*-indol-2-yl)(3,4,5-trimethoxyphenyl)methanone (11d)

Yield: 39.6%. ^{1}H NMR (500 MHz, $CDCl_3$) δ 8.08–8.20 (m, 3H), 7.65–7.72 (m, 1H), 7.56–7.65 (m, 3H), 7.45–7.53 (m, 1H), 7.28–7.35 (m, 2H), 6.92 (s, 1H), 4.02 (s, 3H), 3.94 (s, 6H). MS (ESI) calcd for $C_{24}H_{20}ClNO_6S$ 485.1, found 508.1 $[M+Na]^+$.

8.33. (6-Methyl-1-(phenylsulfonyl)-1*H*-indol-2-yl)(3,4,5-trimethoxyphenyl)methanone (11e)

Yield: 26.4%. ^{1}H NMR (500 MHz, $CDCl_3$) δ 8.19 (d, J = 7.8 Hz, 2H), 8.01 (s, 1H), 7.65–7.70 (m, 1H), 7.48–7.63 (m, 3H), 7.33 (s, 2H), 7.21 (d, J = 8.1 Hz, 1H), 6.98 (s, 1H), 4.02 (s, 3H), 3.92–3.97 (m, 6H), 2.61 (s, 3H). MS (ESI) calcd for $C_{25}H_{23}NO_6S$ 465.1, found 488.0 $[M+Na]^+$.

8.34. (5-Fluoro-1-(phenylsulfonyl)-1*H*-indol-2-yl)(3,4,5-trimethoxyphenyl)methanone (11f)

Yield: 41.5%. ^{1}H NMR (500 MHz, $CDCl_3$) δ 8.15 (d, J = 7.8 Hz, 3H), 7.68 (t, J = 7.3 Hz, 1H), 7.59 (t, J = 7.7 Hz, 2H), 7.22–7.34 (m, 4H), 6.95 (s, 1H), 3.99–4.05 (m, 3H), 3.95 (s, 6H). MS (ESI) calcd for $C_{24}H_{20}FNO_6S$ 469.1, found 492.0 $[M+Na]^+$.

8.35. (1-(Phenylsulfonyl)-1*H*-benzo[*d*]imidazol-2-yl)(3,4,5-trimethoxyphenyl)methanone (11g)

Yield: 15.2%. ^{1}H NMR (500 MHz, $CDCl_3$) δ 8.36 (d, J = 7.6 Hz, 2H), 8.14 (d, J = 8.3 Hz, 1H), 8.07 (d, J = 7.8 Hz, 1H), 7.91 (d, J = 8.1 Hz, 1H), 7.50–7.80 (m, 5H), 7.09 (s, 1H), 4.03 (s, 3H), 3.96 (s, 6H). MS (ESI) calcd for $C_{23}H_{20}N_2O_6S$ 452.1, found 475.0 $[M+Na]^+$.

8.36. (5-Methoxy-1-(phenylsulfonyl)-1*H*-indol-2-yl)(3,4,5-trimethoxyphenyl)methanone (11h)

Yield: 32.1%; ^{1}H NMR (500 MHz, $CDCl_3$) δ 8.03–8.07 (m, 4H), 7.60 (t, J = 7.5 Hz, 1H), 7.51 (t, J = 7.5 Hz, 2H), 7.25 (s, 1H), 7.09 (dd, J = 9.0 Hz, 2.0 Hz, 1H), 7.00 (d, J = 2.5 Hz, 1H), 6.89 (s, 1H), 3.97 (s, 3H), 3.90 (s, 6H), 3.85 (s, 3H). MS (ESI) calcd for $C_{25}H_{23}NO_7S$ 481.1, found 504.1 $[M+Na]^+$.

8.37. (6-Chloro-1*H*-indol-2-yl)(3,4,5-trimethoxyphenyl)methanone (12a)

Yield: 76.8%; mp 207–209 °C. ^{1}H NMR ($CDCl_3$, 500 MHz) δ 9.37 (s, 1H), 7.72 (d, J = 8.5 Hz, 1H), 7.56 (s, 1H), 7.32 (s, 2H), 7.21–7.23 (m, 2H), 4.03 (s, 3H), 4.02 (s, 6H). MS (ESI) calcd for $C_{18}H_{16}ClNO_4$ 345.1, found 368.0 $[M+Na]^+$. HPLC1: t_R 4.32 min, purity >99%.

8.38. (6-Fluoro-1*H*-indol-2-yl)(3,4,5-trimethoxyphenyl)methanone (12b)

Yield: 82.5%; mp 202–204 °C. ^{1}H NMR ($CDCl_3$, 500 MHz) δ 9.32 (s, 1H), 7.74 (q, J = 5.0 Hz, 1H), 7.32 (s, 2H), 7.20–7.23 (m, 2H), 7.03 (dt, J = 9.0 Hz, 2.0 Hz, 1H), 4.03 (s, 3H), 4.02 (s, 6H). MS (ESI) calcd for $C_{18}H_{16}FNO_4$ 329.1, found 352.0 $[M+Na]^+$, 327.9 $[M-H]^-$. HPLC1: t_R 4.27 min, purity 98.7%.

8.39. (6-Methoxy-1*H*-indol-2-yl)(3,4,5-trimethoxyphenyl)-methanone (12c)

Yield: 86.9%; mp 167–169 °C. ^{1}H NMR ($CDCl_3$, 500 MHz) δ 9.06 (s, 1H), 7.52 (d, J = 9.0 Hz, 1H), 7.17 (s, 2H), 7.06 (s, 1H), 6.77–6.80 (m, 2H), 3.88 (s, 3H), 3.87 (s, 6H), 3.82 (s, 3H). MS (ESI) calcd for $C_{19}H_{19}NO_5$ 341.1, found 364.1 $[M+Na]^+$. HPLC2: t_R 4.21 min, purity 97.4%.

8.40. (5-Chloro-1*H*-indol-2-yl)(3,4,5-trimethoxyphenyl)-methanone (12d)

Yield: 87.2%; mp 252–254 °C. ^{1}H NMR (DMSO-d_6, 500 MHz) δ 12.20 (s, 1H), 7.83 (s, 1H), 7.56 (d, J = 8.5 Hz, 1H), 7.36 (d, J = 8.5 Hz, 1H), 7.27–7.30 (m, 3H), 3.93 (s, 6H), 3.84 (s, 3H). MS (ESI) calcd for $C_{18}H_{16}ClNO_4$ 345.1, found 368.1 [M+Na]$^+$. HPLC1: t_R 17.3 min, purity >99%.

8.41. (6-Methyl-1*H*-indol-2-yl)(3,4,5-trimethoxyphenyl)methanone (12e)

Yield: 90.1%; mp 179–181 °C. ^{1}H NMR ($CDCl_3$, 500 MHz) δ 9.37 (s, 1H), 7.67 (d, J = 8.5 Hz, 1H), 7.32–7.33 (m, 3H), 7.20 (s, 1H), 7.08 (d, J = 8.5 Hz, 1H), 4.02 (s, 3H), 4.01 (s, 6H), 2.57 (s, 3H). MS (ESI) calcd for $C_{19}H_{19}NO_4$ 345.1, found 368.0 [M+Na]$^+$. HPLC1: t_R 4.14 min, purity >99%.

8.42. (5-Fluoro-1*H*-indol-2-yl)(3,4,5-trimethoxyphenyl)methanone (12f)

Yield: 69.8%; mp 196–198 °C. ^{1}H NMR ($CDCl_3$, 500 MHz) δ 9.34 (s, 1H), 7.50 (q, J = 4.5 Hz, 1H), 7.43 (dd, J = 8.5 Hz, 2.0 Hz, 1H), 7.33 (s, 2H), 7.20–7.24 (m, 2H), 4.03 (s, 3H), 4.02 (s, 6H). MS (ESI) calcd for $C_{18}H_{16}FNO_4$ 329.1, found 352.0 [M+Na]$^+$, 327.9 [M−H]$^-$. HPLC1: t_R 4.10 min, purity >99%.

8.43. (1*H*-Benzo[*d*]imidazol-2-yl)(3,4,5-trimethoxyphenyl)-methanone (12g)

Yield: 12.7%; mp 191–193 °C. ^{1}H NMR ($CDCl_3$, 500 MHz) δ 10.43 (s, 1H), 8.20 (s, 2H), 7.99 (br, 1H), 7.68 (br, 1H), 7.49 (s, 2H), 4.07 (s, 6H), 4.04 (s, 3H). MS (ESI) calcd for $C_{17}H_{16}N_2O_4$ 312.1, found 310.9 [M−H]$^-$. HPLC1: t_R 4.30 min, purity >99%.

8.44. (5-Methoxy-1*H*-indol-2-yl)(3,4,5-trimethoxyphenyl)-methanone (12h)

Yield: 96.3%; mp 215–217 °C. ^{1}H NMR (DMSO, 500 MHz) δ 11.81 (s, 1H), 7.89 (d, J = 9.0 Hz, 1H), 7.22 (s, 2H), 7.15–7.16 (m, 2H), 6.97 (dd, J = 9.0 Hz, 2.5 Hz, 1H), 3.88 (s, 6H), 3.78 (s, 3H), 3.77 (s, 3H). MS (ESI) calcd for $C_{19}H_{19}NO_5$ 341.1, found 339.9 [M−H]$^-$. HPLC2: t_R 4.18 min, purity >99%.

8.45. (6-Chloro-1-methyl-1*H*-indol-2-yl)(3,4,5-trimethoxyphenyl)methanone (13aa)

Yield: 85.3%; mp 123–125 °C. ^{1}H NMR ($CDCl_3$, 500 MHz) δ 7.67 (d, J = 8.0 Hz, 1H), 7.51 (s, 1H), 7.33 (s, 2H), 7.21 (d, J = 8.0 Hz, 1H), 7.08 (s, 1H), 4.12 (s, 3H), 4.02 (s, 3H), 3.98 (s, 6H). MS (ESI) calcd for $C_{19}H_{18}ClNO_4$ 359.1, found 382.0 [M+Na]$^+$. HPLC2: t_R 9.3 min, purity 98.6%.

8.46. (1-Benzyl-6-chloro-1*H*-indol-2-yl)(3,4,5-trimethoxyphenyl)methanone (13ab)

Yield: 73.4%; liquid. ^{1}H NMR ($CDCl_3$, 500 MHz) δ 7.70 (d, J = 8.0 Hz, 1H), 7.48 (s, 1H), 7.41–7.43 (m, 2H), 7.28–7.37 (m, 2H), 7.17–7.23 (m, 5H), 5.83 (s, 2H), 4.02 (s, 3H), 3.96 (s, 6H). MS (ESI) calcd for $C_{25}H_{22}ClNO_4$ 435.1, found 458.0 [M+Na]$^+$. HPLC1: t_R 10.2 min, purity >99%.

8.47. (6-Fluoro-1-methyl-1*H*-indol-2-yl)(3,4,5-trimethoxyphenyl)methanone (13b)

Yield: 50.8%; mp 98–100 °C. ^{1}H NMR ($CDCl_3$, 500 MHz) δ 7.69 (q, J = 8.5 Hz, 1H), 7.26 (s, 2H), 7.02–7.17 (m, 3H), 4.11 (s, 3H), 4.02 (s, 3H), 3.97 (s, 6H). MS (ESI) calcd for $C_{19}H_{18}FNO_4$ 343.1, found 344.0 [M+H]$^+$. HPLC2: t_R 4.19 min, purity >99%.

8.48. Benzo[*d*]thiazol-2-yl(3,4,5-trimethoxyphenyl)methanone (15a)

Yield: 8.4%; mp 144–146 °C. ^{1}H NMR ($CDCl_3$, 500 MHz) δ 8.29 (d, J = 8.0 Hz, 1H), 8.09 (d, J = 7.5 Hz, 1H), 8.03 (s, 2H), 7.63–7.67 (m, 2H), 4.06 (s, 6H), 4.04 (s, 3H). MS (ESI) calcd for $C_{17}H_{15}N_2O_4S$ 329.1, found 352.1 [M+Na]$^+$. HPLC1: t_R 17.5 min, purity 95.2%.

8.49. Bis(benzo[*d*]thiazol-2-yl)(3,4,5-trimethoxyphenyl)-methanol (15aa)

Yield: 40.5%; mp 50–52 °C. ^{1}H NMR ($CDCl_3$, 500 MHz) δ 8.10 (d, J = 8.0 Hz, 2H), 7.95 (d, J = 8.0 Hz, 2H), 7.55 (t, J = 7.0 Hz, 2H), 7.46 (t, J = 7.5 Hz, 2H), 7.23 (s, 2H), 6.22 (s, 1H), 3.90 (s, 6H), 3.88 (s, 3H). MS (ESI) calcd for $C_{24}H_{20}N_2O_4S_2$ 464.1, found 487.1 [M+Na]$^+$. HPLC2: t_R 3.99 min, purity 98.8%.

8.50. Benzo[*d*]oxazol-2-yl(3,4,5-trimethoxyphenyl)methanone (15b)

Yield: 22.5%; mp 89–91 °C. ^{1}H NMR ($CDCl_3$, 500 MHz) δ 7.81–7.83 (m, 1H), 7.48–7.58 (m, 3H), 7.32–7.43 (m, 2H), 4.06 (s, 3H), 4.01 (s, 6H). MS (ESI) calcd for $C_{17}H_{15}NO_5$ 313.1, found 336.1 [M+Na]$^+$. HPLC2: t_R 4.13 min, purity >97.2%.

8.51. 1-(Phenylsulfonyl)-1*H*-indole-5-carbaldehyde (17)

^{1}H NMR (500 MHz, $CDCl_3$) Yield: 32.6% δ 10.17 (s, 1H), 8.25–8.39 (m, 2H), 7.97–8.09 (m, 3H), 7.69 (t, J = 7.33 Hz, 1H), 7.59 (t, J = 7.5 Hz, 2H), 7.39–7.54 (m, 2H). MS (ESI) calcd for $C_{15}H_{11}NO_3S$ 285.1, found 286.0 [M+H]$^+$.

8.52. 5-(1*H*-Imidazol-2-yl)-1-(phenylsulfonyl)-1*H*-indole (18)

^{1}H NMR (500 MHz, DMSO-d_6) Yield: 12.0% δ 8.33 (d, J = 2.9 Hz, 2H), 8.13 (d, J = 7.8 Hz, 2H), 7.98–8.04 (m, 1H), 7.62–7.67 (m, 1H), 7.55 (d, J = 7.82 Hz, 2H), 7.22–7.34 (m, 4H). MS (ESI) calcd for $C_{17}H_{13}N_3O_2S$ 323.1, found 324.0 [M+H]$^+$.

8.53. 1-(Phenylsulfonyl)-5-(1-(phenylsulfonyl)-1*H*-imidazol-2-yl)-1*H*-indole (19)

Yield: 23.6%. ^{1}H NMR ($CDCl_3$, 500 MHz) δ 8.01 (d, J = 8.5 Hz, 1H), 7.95 (d, J = 7.5 Hz, 2H), 7.73 (d, J = 1.0 Hz, 1H), 7.70 (d, J = 4.0 Hz, 1H), 7.63–7.66 (m, 2H), 7.52–7.56 (m, 3H), 7.31–7.34 (m, 3H), 7.22 (t, J = 8.5 Hz, 2H), 7.17 (s, 1H), 6.14 (d, J = 3.5 Hz, 1H). MS (ESI) calcd for $C_{23}H_{17}N_3O_4S_2$ 463.1, found 464.0 [M+H]$^+$.

8.54. (1-(Phenylsulfonyl)-2-(1-(phenylsulfonyl)-2-(3,4,5-trimethoxybenzoyl)-1*H*-indol-5-yl)-1*H*-imidazol-4-yl)(3,4,5-trimethoxyphenyl)methanone (20b)

Yield: 15.9%. ^{1}H NMR (500 MHz, $CDCl_3$) δ 8.18–8.25 (m, 3H), 8.04 (d, J = 8.1 Hz, 2H), 7.70–7.78 (m, 2H), 7.61–7.69 (m, 3H), 7.55 (t, J = 7.7 Hz, 3H), 7.50 (s, 1H), 7.38 (s, 2H), 7.34 (s, 2H), 6.94 (s, 1H), 3.99–4.06 (m, 12H), 3.94–3.99 (m, 6H). MS (ESI) calcd for $C_{43}H_{37}N_3O_{12}S_2$ 851.2, found 852.1 [M+H]$^+$.

8.55. (5-(4-(3,4,5-Trimethoxybenzoyl)-1*H*-imidazol-2-yl)-1*H*-indol-2-yl)(3,4,5-trimethoxyphenyl)methanone (21b)

Yield: 45.9%; mp 239–241 °C. ^{1}H NMR ($CDCl_3$, 500 MHz) δ 10.45 (s, 1H), 9.44 (s, 1H), 8.41 (s, 1H), 8.04 (d, J = 8.5 Hz, 1H), 7.86 (s, 1H),

7.61 (d, J = 8.5 Hz, 1H), 7.26–7.29 (m, 5H), 3.99 (s, 3H), 3.95–3.97 (m, 15H). MS (ESI) calcd for $C_{31}H_{29}N_3O_8$ 571.2, found 572.2 $[M+H]^+$. HPLC2: t_R 4.09 min, purity 96.3%.

8.56. Cell culture and cytotoxicity assay

We examined the antiproliferative activity of the ABI-II compounds in two melanoma cell lines (A375 and WM-164) and four human prostate cancer cell lines (LNCaP, DU 145, PC-3, and PPC-1). These cell lines were purchased from ATCC (American Type Culture Collection, Manassas, VA) except the PPC-1 cell line, which was kindly provided by Dr. Mitchell Steiner at the University of Tennessee Health Science Center. The Pgp overexpressing multidrug resistant cell line MDA-MB-435/LCC6MDRI and matching sensitive parent cell line were kindly provided by Dr. Robert Clarke (Georgetown University, Washington, DC). Paclitaxel-resistant PC-3-TxR, DU145-TxR, and their parental cell lines were gifts from Dr. Evan Keller at the University of Michigan. Melanoma cells were cultured in DMEM (Cellgro Mediatech, Inc., Herndon, VA), and prostate cancer cells were cultured in RPMI 1640 (Cellgro Mediatech, Inc.,) supplemented with 10% FBS (Cellgro Mediatech). Cultures were maintained at 37 °C in a humidified atmosphere containing 5% CO_2. Cells (1000–5000) were plated into each well of 96-well plates depending on growth rate and exposed to different concentrations of a test compound for 48 h (fast growing melanoma cells) or 96 h (slow growing prostate cancer cells) in three to five replicates. Cell numbers at the end of the drug treatment were measured by the sulforhodamine B (SRB) assay. Briefly, the cells were fixed with 10% trichloroacetic acid and stained with 0.4% SRB, and the absorbances at 540 nm were measured using a plate reader (DYNEX Technologies, Chantilly, VA). Percentages of cell survival versus drug concentrations were plotted, and the IC_{50} (concentration that inhibited cell growth by 50% of untreated control) values were obtained by nonlinear regression analysis using GraphPad Prism (GraphPad Software, San Diego, CA).

8.57. In vitro metabolic stability

Metabolic stability studies were conducted by incubating 0.5 μM of test compounds in a total reaction volume of 1 ml containing 1 mg/mL microsomal protein in reaction buffer [0.2 M of phosphate buffer solution (pH 7.4), 1.3 mM $NADP^+$, 3.3 mM glucose-6-phosphate, and 0.4 U/mL glucose-6-phosphate dehydrogenase] at 37 °C in a shaking water bath. The compound **3ab**, at 50 μM concentration, with the above mentioned conditions, was used for metabolite identification studies. The NADPH regenerating system (solutions A and B) was obtained from BD Biosciences (Bedford, MA). The total DMSO concentration in the reaction solution was approximately 0.5% (v/v). Aliquots (100 μL) from the reaction mixtures used to determine metabolic stability were sampled at 5, 10, 20, 30, 60, and 90 min. Acetonitrile (150 μL) containing 200 nM of the internal standard was added to quench the reaction and to precipitate the proteins. Samples were then centrifuged at 4000g for 30 min at room temperature, and the supernatant was analyzed directly by liquid chromatography–tandem mass spectrography.

8.58. In vitro microtubule polymerization assay

Bovine brain tubulin (0.4 mg) (Cytoskeleton, Denver, CO) was mixed with 5, 10, 20 μM of the test compounds or colchicine (positive control) and incubated in 110 μL of general tubulin buffer (80 mM PIPES, 2.0 mM $MgCl_2$, 0.5 mMEGTA, and 1 mM GTP) at pH 6.9. The absorbance at 340 nm was monitored every 1 min for 15 min by the SYNERGY 4 microplate reader (Bio-Tek Instruments, Winooski, VT). The spectrophotometer was set at 37 °C for tubulin polymerization.

8.59. Molecular modeling

All molecular modeling studies were performed with Schrodinger Molecular Modeling Suite 2010 (Schrodinger LLC, New York, NY) running on a Dell Linux workstation. We selected tubulin complex with TN16 (PDB code: 3HKD) as our modeling system because of the structure similarity between ABI-II analogs and TN16. ABI-IIs were built and prepared using the Ligprep module, and they were docked into the TN16 site by the Glide module in the Schrodinger Suite. The best docking complexes were subject to restricted molecular dynamics to release any strains by using the Macromodel module with OPLS-2005 force field. The ligand and its surrounding residues within 15 Å were allowed to move freely, while residues outside the 15 Å radius were kept rigid.

Acknowledgements

The project was supported by Grant Number 1R01CA148706-01A1 from NIH/NCI. The contents are solely the responsibility of the authors and do not necessarily represent the official views of the NIH. Additional support came from GTx, Inc. We thank Dr. Ryan Yates for providing access to an HPLC instrument. We also thank Dr. David Armbruster, University of Tennessee Health Science Center, and Dr. Michael L. Mohler from GTx, Inc., for editorial assistance.

Supplementary data

Supplementary data associated with this article can be found, in the online version, at doi:10.1016/j.bmc.2011.06.084.

References and notes

1. Heron, M.; Hoyert, D. L.; Murphy, S. L.; Xu, J.; Kochanek, K. D.; Tejada-Vera, B. *Natl. Vital Stat. Rep.* **2009**, *57*, 1.
2. ClinicalTrials.gov. ClinicalTrials.gov Identifier, NCT00653939, 2009.
3. ClinicalTrials.gov. Clinical Trials.gov Identifier Number, NCT00003768, 2010.
4. Fox, E.; Maris, J. M.; Widemann, B. C.; Goodspeed, W.; Goodwin, A.; Kromplewski, M.; Fouts, M. E.; Medina, D.; Cohn, S. L.; Krivoshik, A.; Hagey, A. E.; Adamson, P. C.; Balis, F. M. *Clin. Cancer Res.* **2008**, *14*, 1111.
5. Gottesman, M. M.; Fojo, T.; Bates, S. E. *Nat. Rev. Cancer* **2002**, *2*, 48.
6. Colabufo, N. A.; Pagliarulo, V.; Berardi, F.; Contino, M.; Inglese, C.; Niso, M.; Ancona, P.; Albo, G.; Pagliarulo, A.; Perrone, R. *Eur. J. Pharmacol.* **2008**, *601*, 38.
7. Volm, M.; Mattern, J. *Crit. Rev. Oncog.* **1996**, *7*, 227.
8. Ojima, I.; Borella, C. P.; Wu, X.; Bounaud, P. Y.; Oderda, C. F.; Sturm, M.; Miller, M. L.; Chakravarty, S.; Chen, J.; Huang, Q.; Pera, P.; Brooks, T. A.; Baer, M. R.; Bernacki, R. J. *J. Med. Chem.* **2005**, *48*, 2218.
9. Bhandari, M. S.; Hussain, M. *BJU Int.* **2005**, *96*, 296.
10. Chen, J.; Wang, Z.; Li, C.-M.; Lu, Y.; Vaddady, P. K.; Meibohm, B.; Dalton, J. T.; Miller, D. D.; Li, W. *J. Med. Chem.* **2010**, *53*, 7414.
11. Lu, Y.; Li, C. M.; Wang, Z.; Ross, C. R., 2nd; Chen, J.; Dalton, J. T.; Li, W.; Miller, D. D. *J. Med. Chem.* **2009**, *52*, 1701.
12. Li, C.-M.; Chen, J.; Lu, Y.; Narayanan, R.; Parke, D. N.; Li, W.; Miller, D. D.; Dalton, J. T. *Drug Metabolism & Disposition* **2011**, in press.
13. Nien, C. Y.; Chen, Y. C.; Kuo, C. C.; Hsieh, H. P.; Chang, C. Y.; Wu, J. S.; Wu, S. Y.; Liou, J. P.; Chang, J. Y. *J. Med. Chem.* **2010**, *53*, 2309.
14. Mahboobi, S.; Pongratz, H.; Hufsky, H.; Hockemeyer, J.; Frieser, M.; Lyssenko, A.; Paper, D. H.; Burgemeister, J.; Bohmer, F. D.; Fiebig, H. H.; Burger, A. M.; Baasner, S.; Beckers, T. *J. Med. Chem.* **2001**, *44*, 4535.
15. Davies, H. M. L.; Dai, X. *J. Org. Chem.* **2005**, *70*, 6680.
16. Chen, J.; Wang, Z.; Lu, Y.; Dalton, J. T.; Miller, D. D.; Li, W. *Bioorg. Med. Chem. Lett.* **2008**, *18*, 3183.
17. Li, C.-M.; Lu, Y.; Narayanan, R.; Miller, D. D.; Dalton, J. T. *Drug Metab. Dispos.* **2010**, *38*, 2032.
18. Geney, R.; Ungureanu, M.; Li, D.; Ojima, I. *Clin. Chem. Lab. Med.* **2002**, *40*, 918.
19. Dumontet, C.; Sikic, B. I. *J. Clin. Oncol.* **1999**, *17*, 1061.
20. Verrills, N. M.; Kavallaris, M. *Curr. Pharm. Des.* **2005**, *11*, 1719.
21. Ross, D. T.; Scherf, U.; Eisen, M. B.; Perou, C. M.; Rees, C.; Spellman, P.; Iyer, V.; Jeffrey, S. S.; Van de Rijn, M.; Waltham, M.; Pergamenschikov, A.; Lee, J. C.; Lashkari, D.; Shalon, D.; Myers, T. G.; Weinstein, J. N.; Botstein, D.; Brown, P. O. *Nat. Genet.* **2000**, *24*, 227.
22. Dong, X.; Mattingly, C. A.; Tseng, M. T.; Cho, M. J.; Liu, Y.; Adams, V. R.; Mumper, R. J. *Cancer Res.* **2009**, *69*, 3918.
23. Takeda, M.; Mizokami, A.; Mamiya, K.; Li, Y. Q.; Zhang, J.; Keller, E. T.; Namiki, M. *Prostate* **2007**, *67*, 955.

24. Ahn, S., III *C. B. D.; Barrett, C. M.; Hwang, D. J.; Li, C.-M.; Miller, D. D.; Dalton, J. T. Molecular Cancer Therapeutics* **2011**. doi:10.1158/1535-7163.MCT-10-0399.
25. Wang, L.; Woods, K. W.; Li, Q.; Barr, K. J.; McCroskey, R. W.; Hannick, S. M.; Gherke, L.; Credo, R. B.; Hui, Y.-H.; Marsh, K.; Warner, R.; Lee, J. Y.; Zielinski-Mozng, N.; Frost, D.; Rosenberg, S. H.; Sham, H. L. *J. Med. Chem.* **2002**, *45*, 1697.
26. Dorleans, A.; Gigant, B.; Ravelli, R. B.; Mailliet, P.; Mikol, V.; Knossow, M. *Proc. Natl. Acad. Sci. U.S.A.* **2009**, *106*, 13775.